Supplementary Materials:

Nickel complexes based on amidine for applications in gas-assisted methods and photocatalysis

A. Butrymowicz-Kubiak, A. Topolski, T. M. Muzioł, I. B. Szymańska*
Faculty of Chemistry, Nicolaus Copernicus University in Toruń, Gagarina 7, 87-100 Toruń, Poland

*Corresponding authors: E-mail address: Iwona B. Szymańska: Tel.: +48 566114317; e-mail address: pola@umk.pl

Aleksandra Butrymowicz-Kubiak; e-mail address: aleksandra.butrymowicz@doktorant.umk.pl

Table S 1 Crystal data and structure refinement for the compound $[Ni(NHC(CF_3)NC(CF_3)NH)_2]\cdot(NH_4)(NHOCCF_3)\cdot(NH_2OCCF_3)\cdot H_2O$ (**5a**).

Identification code	**(5a)**
Empirical formula	C12 H13 F18 N9 Ni O3
Formula weight	732.02
Temperature [K]	100(2)
Wavelength [Å]	1.54184
Crystal system, space group	Triclinic, P-1
Unit cell dimensions [Å] and [°]	a = 9.04000(18) α = 70.687(2) b = 11.8822(2) β = 79.653(2) c = 12.1180(3) γ = 81.9191(16)
Volume [Å^3]	1203.80(5)
Z, Calculated density [Mg×m^{-3}]	2, 2.017
Absorption coefficient [mm^{-1}]	2.871
F(000)	724
Crystal size [mm^3]	0.090 x 0.060 x 0.040
Theta range for data collection [°]	3.905 to 77.770
Limiting indices	-11<=h<=11 -15<=k<=15 -15<=l<=15
Reflections collected/unique	8742
Completeness [%] to theta [°]	100.0 %
Absorption correction	Analytical
Max. and min. transmission	0.905 and 0.829
Refinement method	Full-matrix least-squares on F^2
Data/restraints/parameters	8742 / 2 / 407
Goodness-of-fit on F^2	1.032
Final R Indices [I>2sigma(I)]	R1 = 0.0415, wR2 = 0.1168
R indices (all data)	R1 = 0.0421, wR2 = 0.1173
Largest diff. peak and hole [eÅ^{-3}]	0.655 and -0.650

Table S 2 Bond lengths [Å] and angles [°] for the compound $[Ni(NHC(CF_3)NC(CF_3)NH)_2]\cdot(NH_4)(NHOCCF_3)\cdot(NH_2OCCF_3)\cdot H_2O$ (**5a**).

Ni(1)-N(1)	1.8587(17)
Ni(1)-N(5)	1.8628(18)
Ni(1)-N(7)	1.8642(18)
Ni(1)-N(3)	1.8633(18)
N(1)-Ni(1)-N(5)	89.93(8)
N(1)-Ni(1)-N(7)	178.42(8)
N(5)-Ni(1)-N(7)	89.97(8)
N(1)-Ni(1)-N(3)	89.66(8)
N(5)-Ni(1)-N(3)	179.59(8)
N(7)-Ni(1)-N(3)	90.43(8)
C(1)-N(1)-Ni(1)	127.61(15)
Ni(1)-N(1)-H(1)	116.2
Ni(1)-N(3)-H(3)	116.2
C(5)-N(5)-Ni(1)	127.09(15)
Ni(1)-N(5)-H(5)	116.5
Ni(1)-N(7)-H(7)	116.3

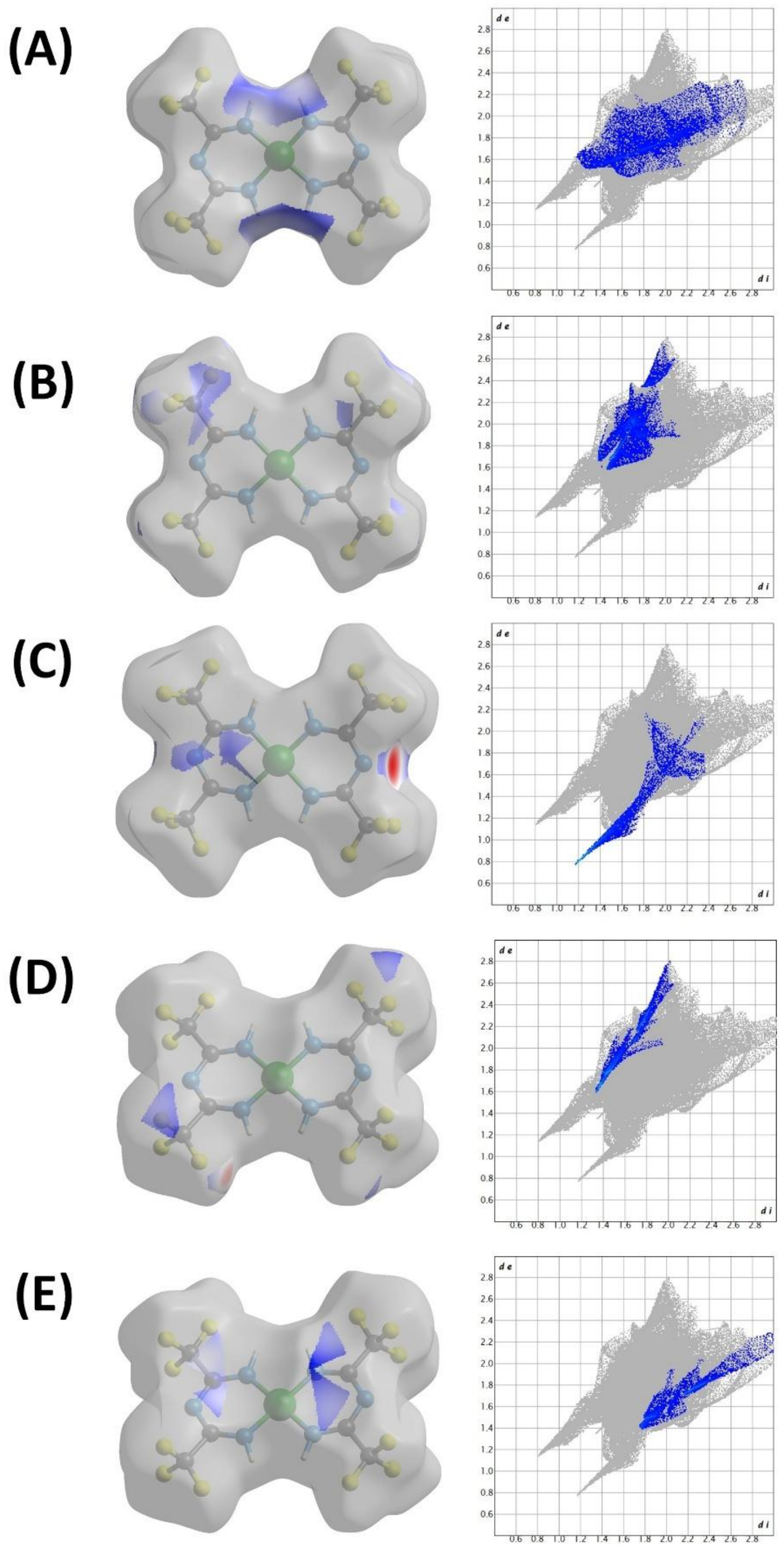

Figure S 1 Hirshfeld surfaces (left) and fingerprints (right) of selected interactions created in the crystal network of $[Ni(NHC(CF_3)NC(CF_3)NH)_2]\cdot(NH_4)(NHOCCF_3)\cdot(NH_2OCCF_3)\cdot H_2O$ (**5a**) for $[Ni(IMAMDCF_3)_2]$ molecule: (A) for H⋯F (4.9%), (B) for F⋯N (4.8%), (C) N⋯H (3.7%), (D) for F⋯C (3.3%), and (E) for C⋯F (2.9%).

Table S 3 Selected IR absorption bands (cm^{-1}) of the studied compounds [$Ni_2(HAMDR_f)_2(\mu$-$O_2CR_f)_4$] (**1−4**).

Compound	νNH*	νCN (sh)	ν_{as}COO	δNH_2	ν_sCOO	ΔνCOO
[$Ni_2(HAMDCF_3)_2(\mu$-$O_2CCF_3)_4$] (1)	3524 3373 3325 3265 3194	1717	1668	1576	1450	218
[$Ni_2(HAMDC_2F_5)_2(\mu$-$O_2CCF_3)_4$] (2)	3514 3373 3325 3271 3206	1715	1668	1566	1456	212
[$Ni_2(HAMDCF_3)_2(\mu$-$O_2CC_2F_5)_4$] (3)	3520 3373 3327 3269 3196	1713	1678	1576	1429	249
[$Ni_2(HAMDC_2F_5)_2(\mu$-$O_2CC_2F_5)_4$] (4)	3526 3375 3323 3244 3198	1713	1680	1551	1429	251
$HAMDCF_3$	3350 3163	1670	−	1575	−	−
$HAMDC_2F_5$	3362 3130	1664	−	1593	−	−

* $\nu_{as}NH_2$, ν_sNH_2, ν=NH

$\Delta\nu CF_3CO_2Na$ = 223 cm^{-1}, $\Delta\nu C_2F_5CO_2Na$ = 268 cm^{-1}; [$Ni_2(\mu$-$O_2CCF_3)_4$] [cm^{-1}]: 1665 ν_{as}COO, 1449 ν_sCOO; [$Ni_2(\mu$-$O_2CC_2F_5)_4$] [cm^{-1}]: 1713, 1641ν_{as}COO, 1431 ν_sCOO

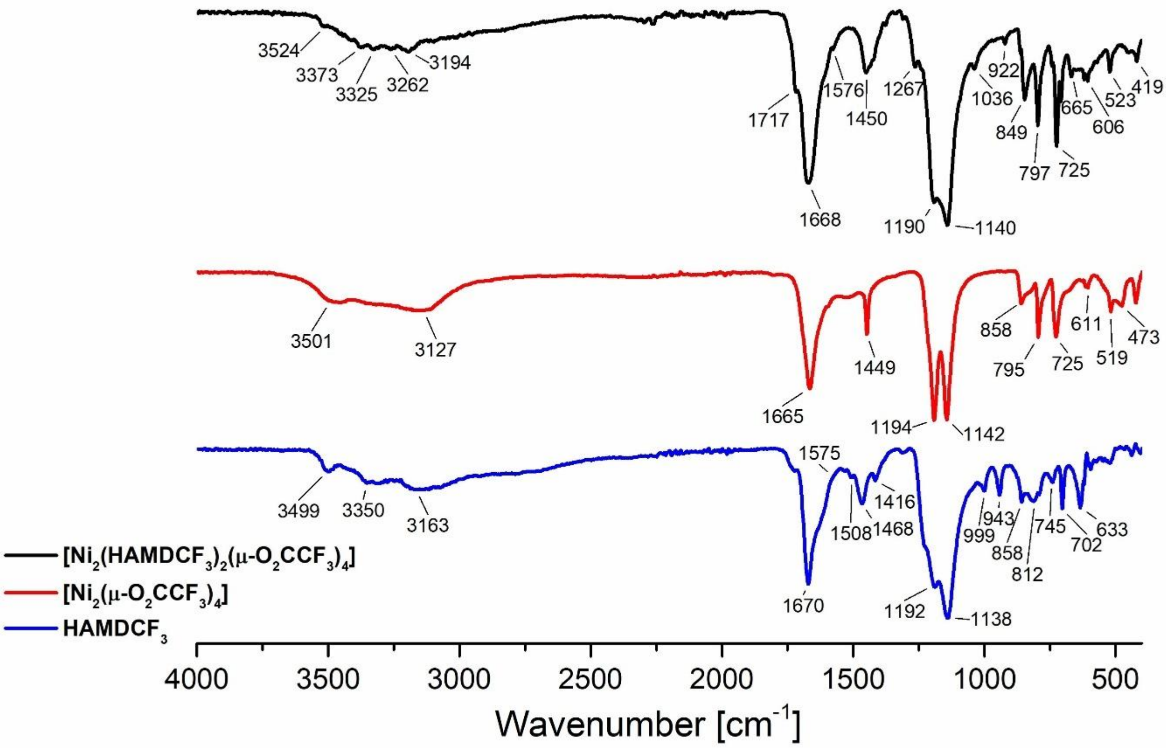

Figure S 2 ATR-IR spectrum for the compound $[Ni_2(HAMDCF_3)_2(\mu\text{-}O_2CCF_3)_4]$ (**1**) (black) and for the reactants $[Ni_2(\mu\text{-}O_2CCF_3)_4]$ (red), $HAMDCF_3$ (blue).

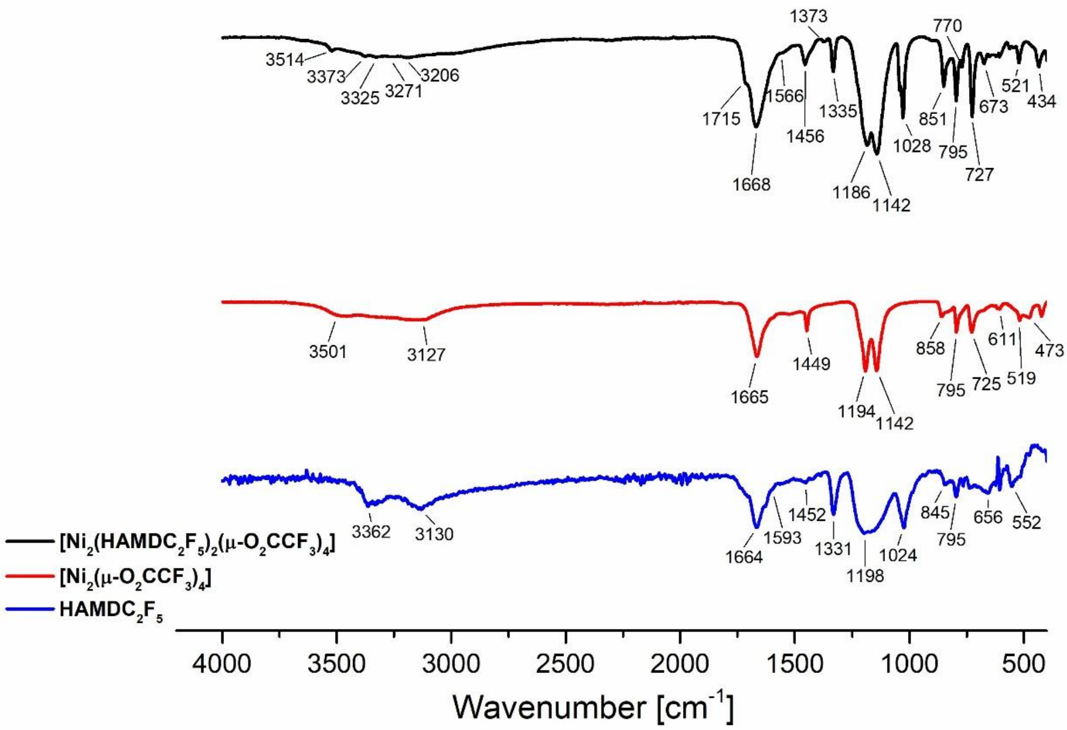

Figure S 3 ATR-IR spectrum for the compound $[Ni_2(HAMDC_2F_5)_2(\mu\text{-}O_2CCF_3)_4]$ (**2**) (black) and for the reactants $[Ni_2(\mu\text{-}O_2CCF_3)_4]$ (red), $HAMDC_2F_5$ (blue).

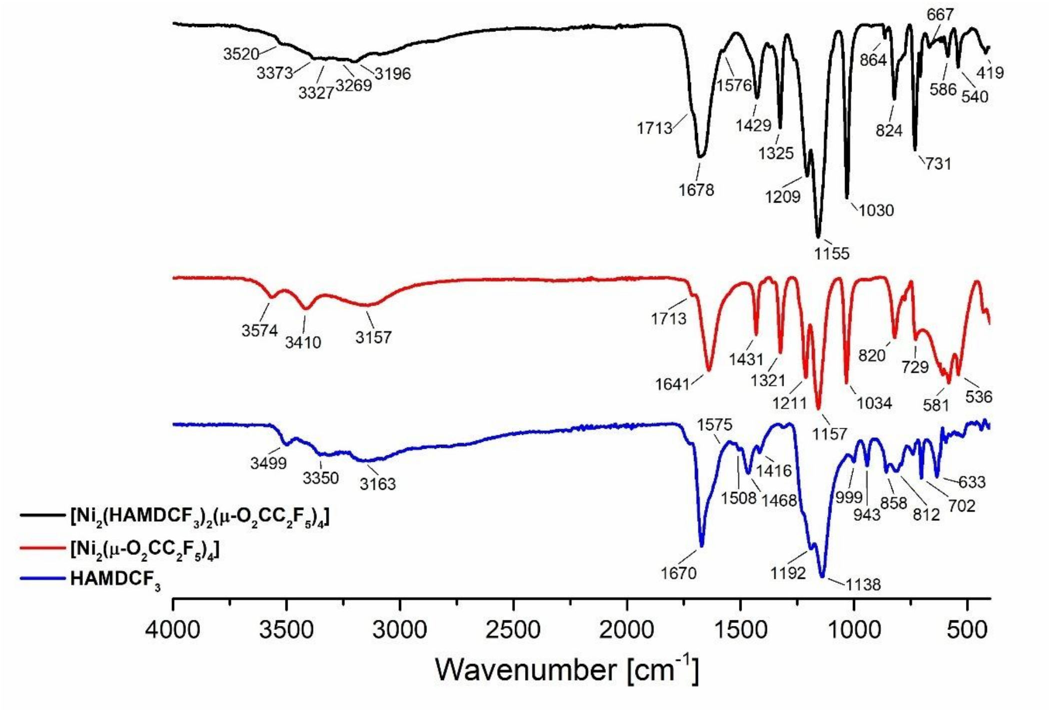

Figure S 4 ATR-IR spectrum for the compound [$Ni_2(HAMDCF_3)_2(\mu\text{-}O_2CC_2F_5)_4$] (**3**) (black) and for the reactants [$Ni_2(\mu\text{-}O_2CC_2F_5)_4$] (red), $HAMDCF_3$ (blue).

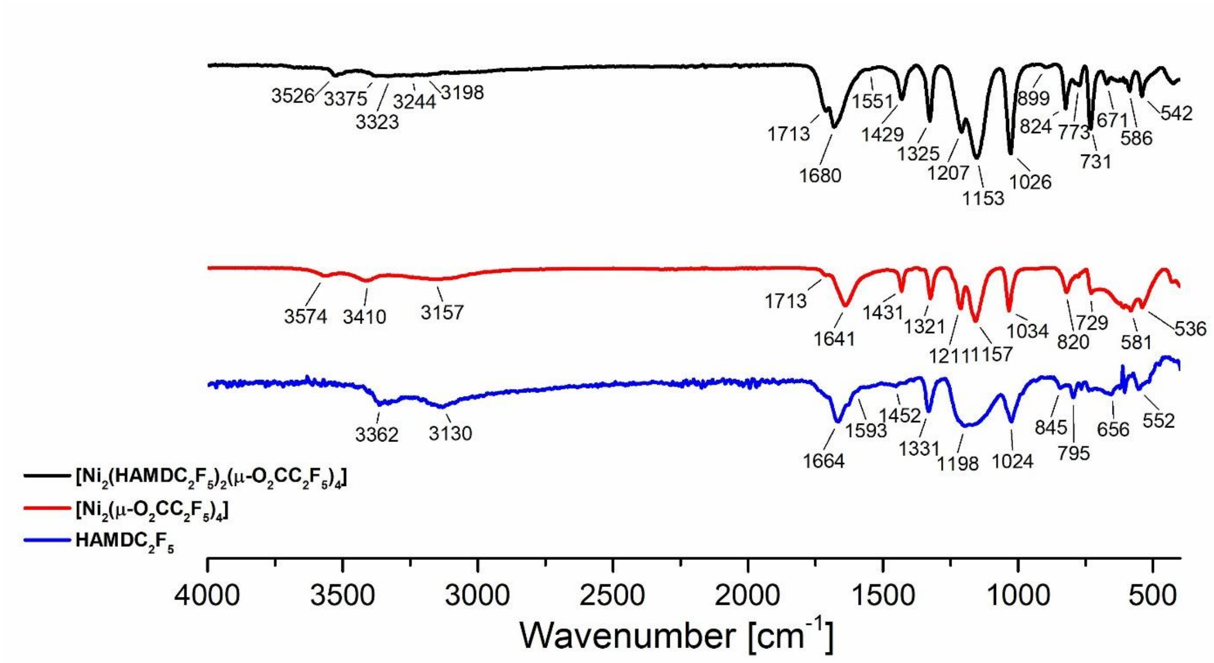

Figure S 5 ATR-IR spectrum for the compound [$Ni_2(HAMDC_2F_5)_2(\mu\text{-}O_2CC_2F_5)_4$] (**4**) (black) and for the reactants [$Ni_2(\mu\text{-}O_2CC_2F_5)_4$] (red), $HAMDC_2F_5$ (blue).

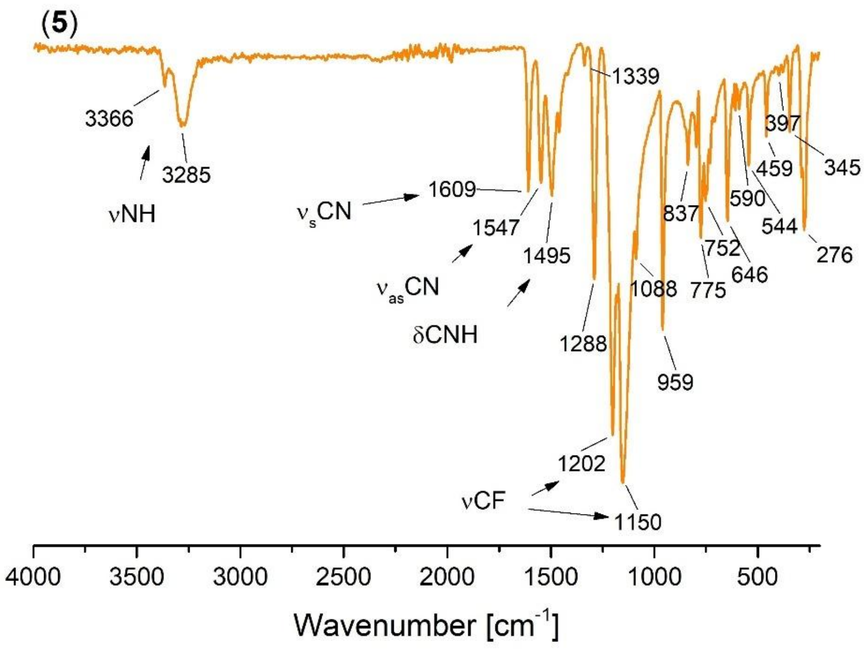

Figure S 6 Infrared spectrum of the [Ni(IMAMDCF_3)$_2$] (**5**).

Table S 4 Thermal analysis results.

Complex	Temperature [K]			Residue [%]	
	T_i	T_m	T_f	Found	Calc.
[Ni_2(HAMDCF_3)$_2$(μ-O_2CCF_3)$_4$] (1)	319 406 529	387 432 445 477 519 597	406 529 620	19.33	14.83 (Ni)
[Ni_2(HAMDC_2F_5)$_2$(μ-O_2CCF_3)$_4$] (2)	320 395 485 528	342 375 474 507 591	395 485 528 623	16.63	13.17 (Ni)
[Ni_2(HAMDCF_3)$_2$(μ-O_2CC_2F_5)$_4$] (3)	313 562	488 601	562 644	5.65	11.82 (Ni)
[Ni_2(HAMDC_2F_5)$_2$(μ-O_2CC_2F_5)$_4$] (4)	320 547	503 600	547 652	4.54	10.74 (Ni)
[Ni(IMAMDCF_3)$_2$] (5)	318 378 423	345 369 413 474	378 423 487	3.97	12.47 (Ni)

T_i, initial temperature; T_m, maximum temperature; T_f, final temperature

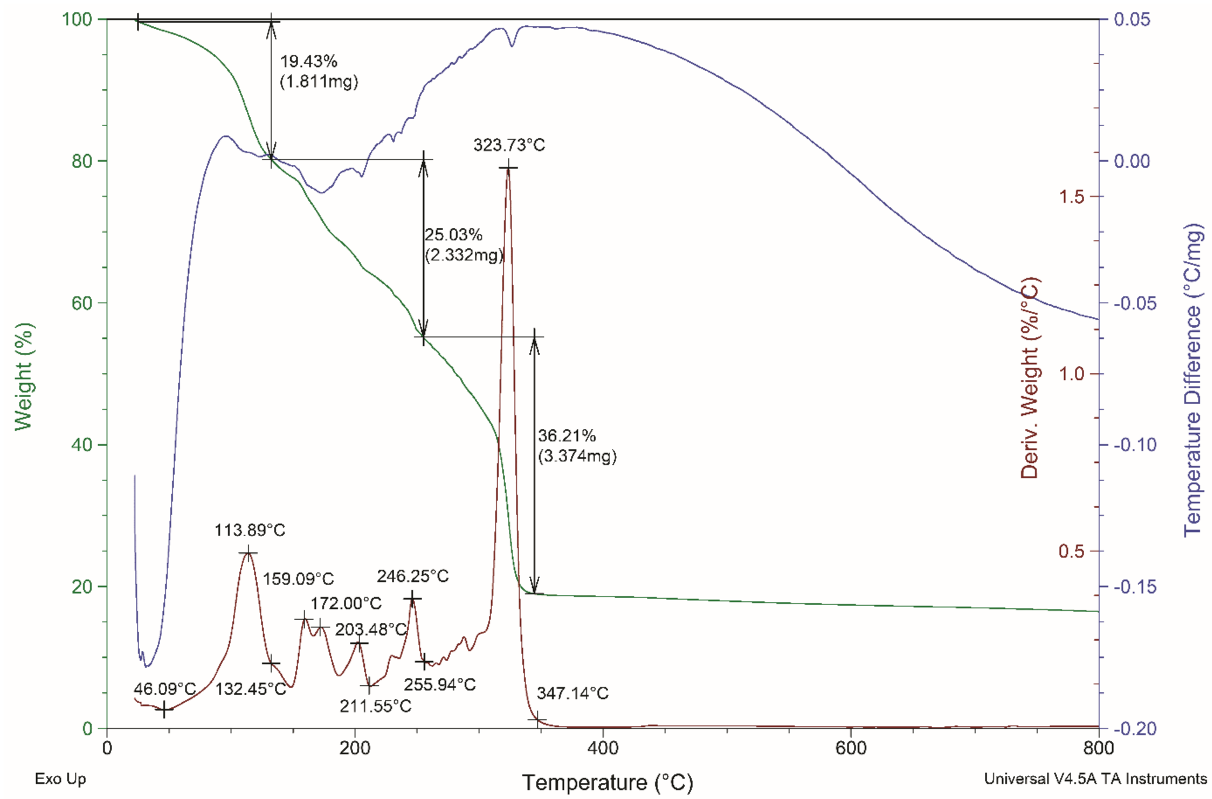

Figure S 7 Thermal decomposition of $[Ni_2(HAMDCF_3)_2(\mu\text{-}O_2CCF_3)_4]$ (**1**) (TG, DTG, DTA curves).

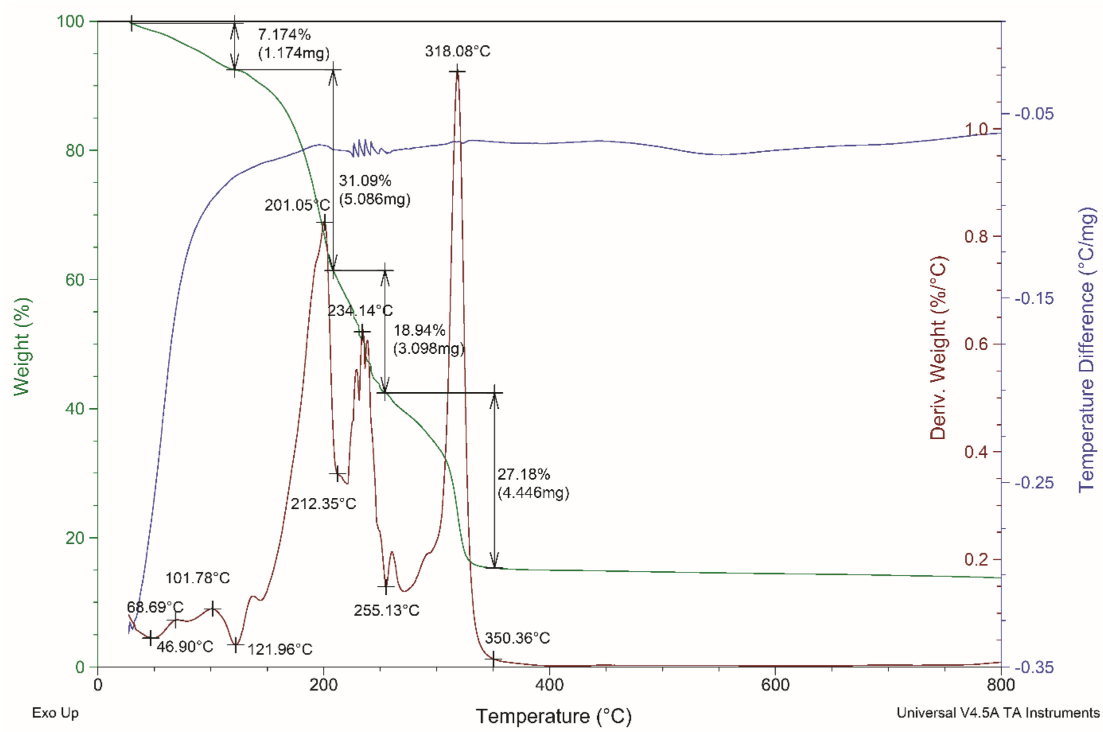

Figure S 8 Thermal decomposition of $[Ni_2(HAMDC_2F_5)_2(\mu\text{-}O_2CCF_3)_4]$ (**2**) (TG, DTG, DTA curves).

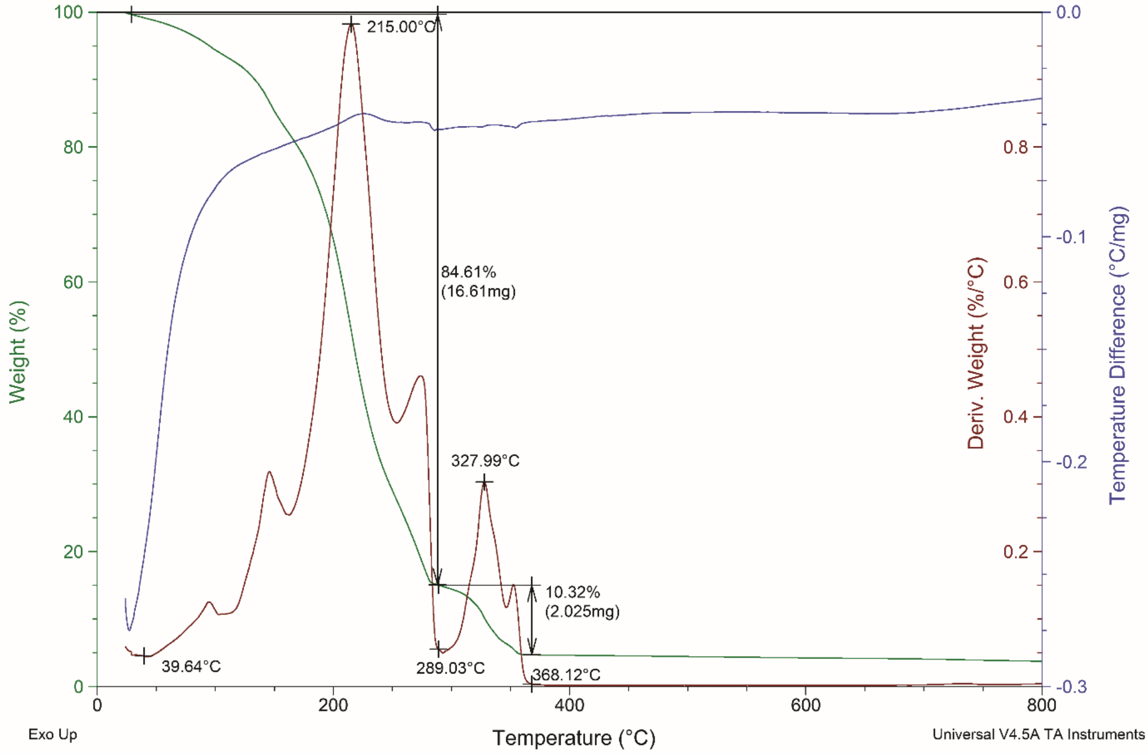

Figure S 9 Thermal decomposition of [$Ni_2(HAMDCF_3)_2(\mu\text{-}O_2CC_2F_5)_4$] (**3**) (TG, DTG, DTA curves).

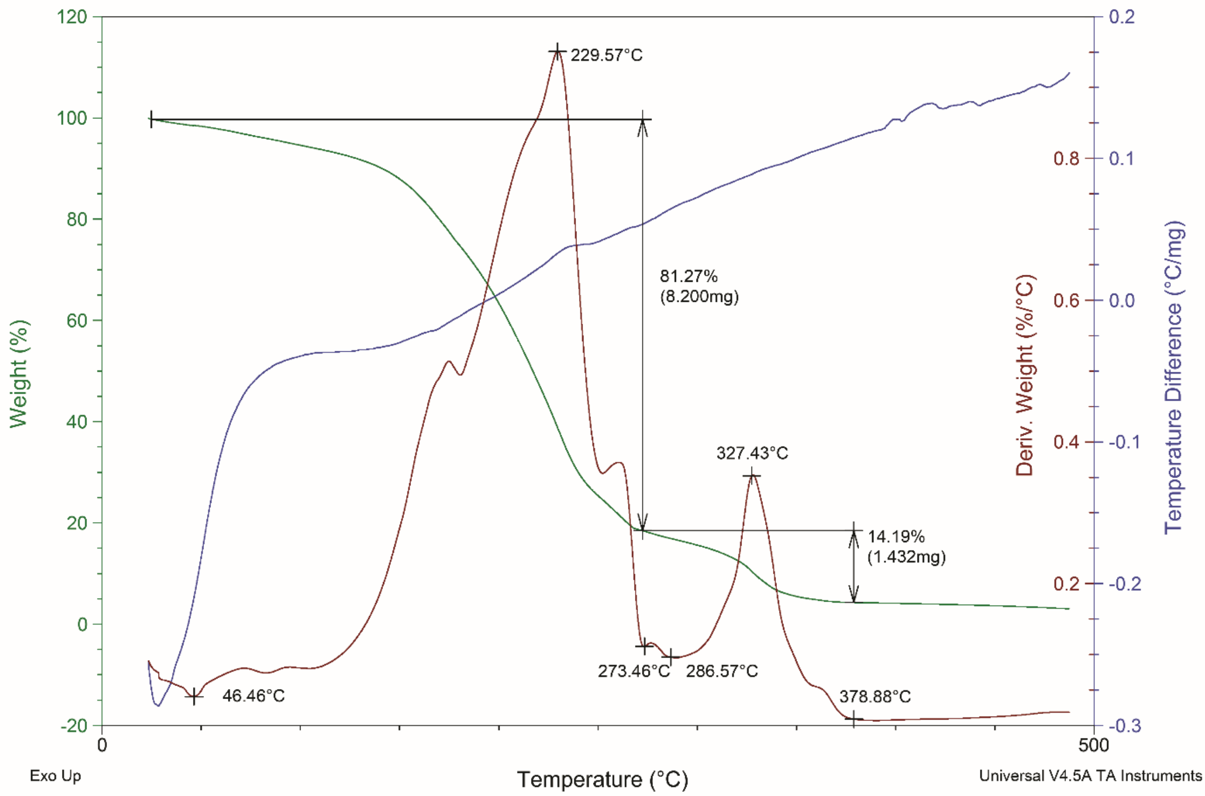

Figure S 10 Thermal decomposition of [$Ni_2(HAMDC_2F_5)_2(\mu\text{-}O_2CC_2F_5)_4$] (**4**) (TG, DTG, DTA curves).

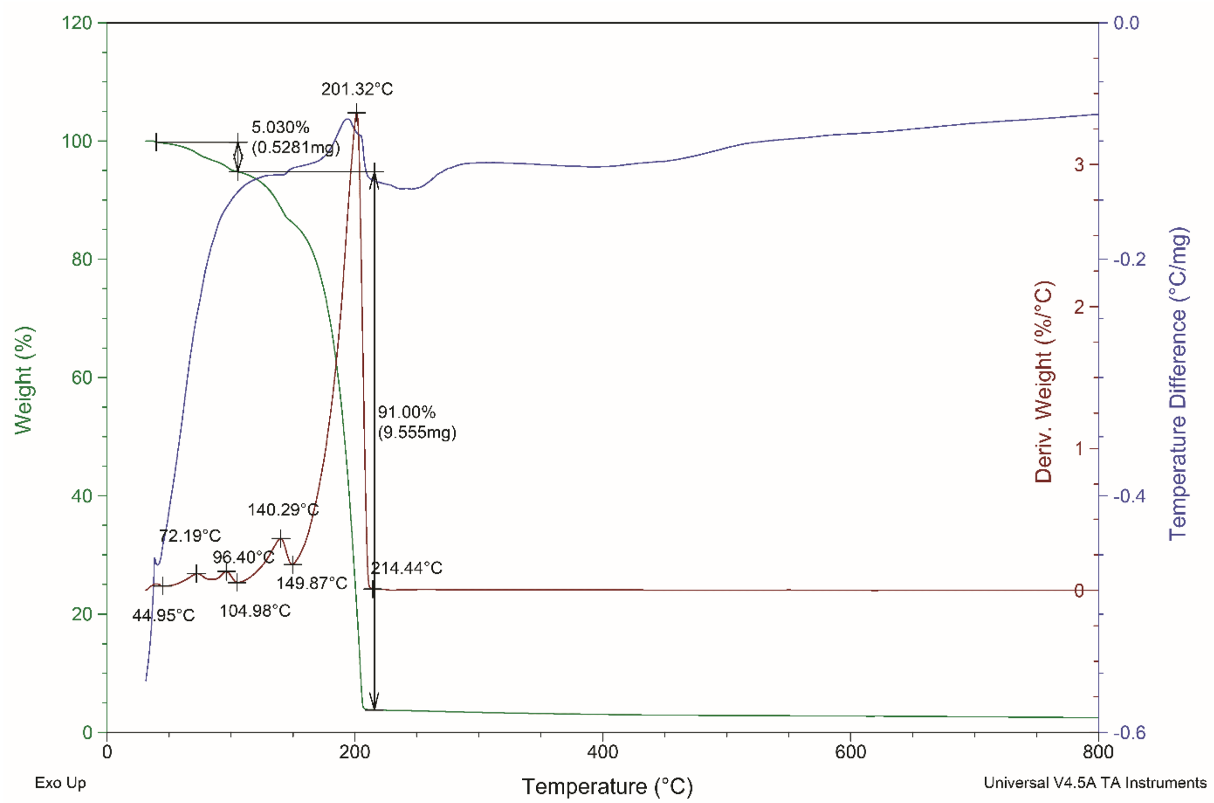

Figure S 11 Thermal decomposition of [Ni(IMAMDCF$_3$)$_2$] (**5**) (TG, DTG, DTA curves).

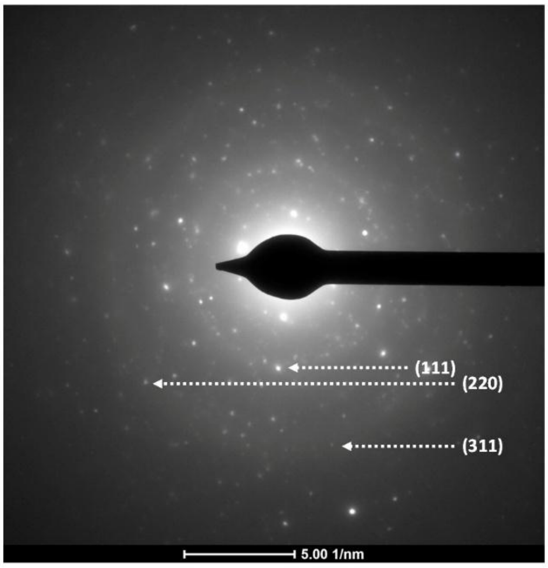

Figure S 12 Transmission electron microscope (TEM) diffraction pattern for the TGA residue (Ni) for [Ni(IMAMDCF$_3$)$_2$] (**5**).

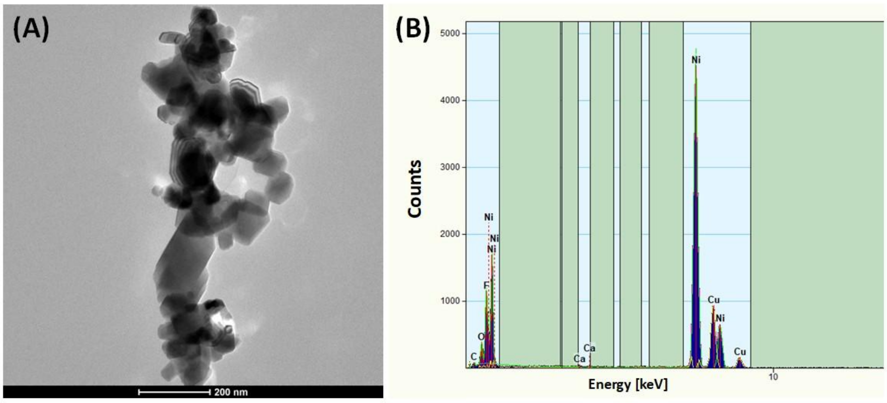

(C)

Element	Atomic content of the element [%at.]
Ni	66.7
F	23.9
O	9.4

Figure S 13 TEM analysis results of the residue after thermal decomposition of $[Ni_2(HAMDCF_3)_2(\mu\text{-}O_2CCF_3)_4]$ (**1**), (A) − TEM image, (B) − EDX spectrum and (C) − atomic content of the elements.

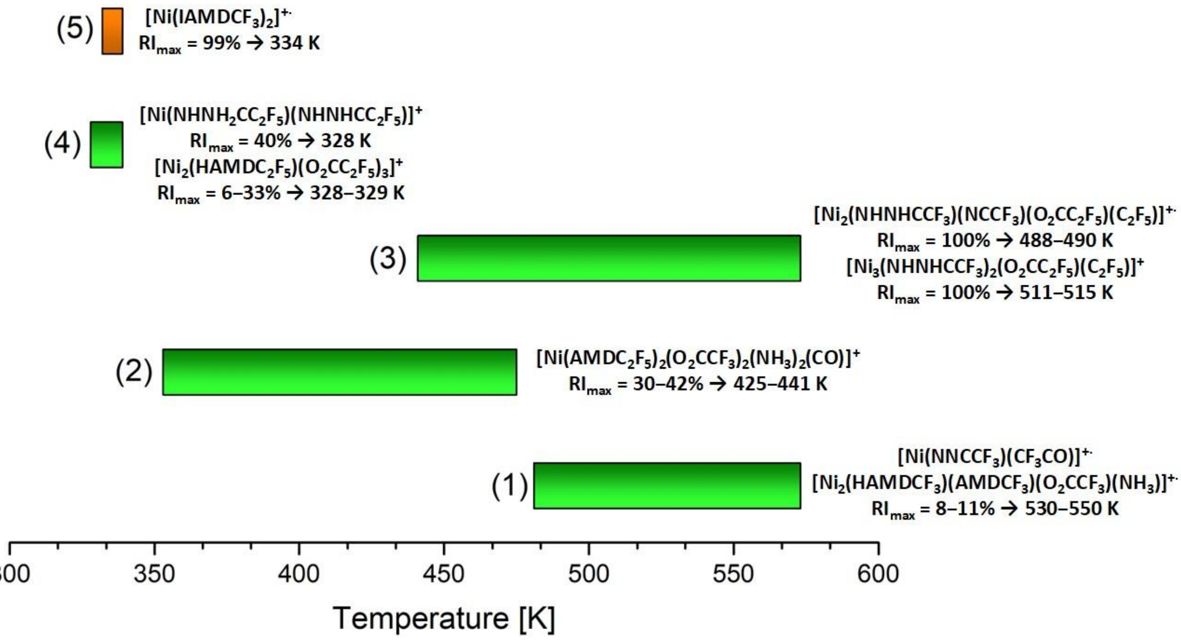

Figure S 14 Temperature ranges for the metallated fragments for compounds (**1−5**). The ions which achieved the highest relative intensity are marked in the diagram.

Table S 5 EI MS results for the complex $[Ni_2(HAMDCF_3)_2(\mu\text{-}O_2CCF_3)_4]$ (**1**).

Fragments	**m/z**	**Relative Intensity (RI) [%]**			
		466 K	**481 K**	**533 K**	**573 K**
$[F_2]^{+\cdot}$	38	–	<1	1	1
$[HN{=}C{=}N]^{+}$	41	1	3	1	1
$[HN{=}C{=}NH]^{+\cdot}$	42	2	9	5	1
$[CO_2]^{+\cdot}$	44	34	52	99	89
$[CO_2H]^{+\cdot}$	45	31	63	36	50
$[Ni]^{+}$	58	–	–	1	<1
$[CF_3]^{+}$	69	100	100	100	100
$[CF_3CN]^{+\cdot}$	95	4	5	3	4
$[CF_3CNH]^{+}$	96	2	3	4	1
$[CF_3CNH_2]^{+\cdot}$	97	3	4	2	4
$[NHNH_2CCF_3]^{+\cdot}$	112	10	16	9	1
$[CF_3CO_2H]^{+\cdot}$	114	1	1	1	1
$[Ni(NHNH_2CCF_3)]^{+}$	170	–	–	2	–
$[Ni(HN{=}C{=}NH)(O_2CCF_3)]^{+}$ $[Ni(NHNHCCF_3)(CO_2)]^{+}$	213	–	–	2	–
$[Ni(NNCCF_3)(CF_3CO)]^{+\cdot}$	264	–	1	11	1
$[Ni_2(NHNH_2CCF_3)(NHNHCCF_3)(O_2CCF_3)(NH_3)]^{+\cdot}$	469	–	1	11	<1
$[Ni_3(NHNHCCF_3)(O_2CCF_3)_2(NH_3)]^{+}$	530	–	–	–	2

Table S 6 EI MS results for the complex $[Ni_2(HAMDC_2F_5)_2(\mu\text{-}O_2CCF_3)_4]$ (**2**).

Fragments	**m/z**	**Relative Intensity (RI) [%]**			
		353 K	**358 K**	**425 K**	**451 K**
$[F_2]^{+\cdot}$	38	<1	1	1	–
$[HN{=}C{=}N]^{+}$	41	4	8	1	–
$[HN{=}C{=}NH]^{+\cdot}$	42	13	15	5	1
$[CO_2]^{+\cdot}$	44	100	100	76	73
$[CO_2H]^{+\cdot}$	45	14	47	28	19
$[Ni]^{+}$	58	1	1	3	–
$[CF_3]^{+}$	69	49	70	100	100
$[CF_2CN]^{+\cdot}$	76	2	3	25	23
$[C_2F_4]^{+}$	100	11	9	8	4
$[CF_3CO_2H]^{+\cdot}$	114	1	1	1	–
$[C_2F_5]^{+}$	119	45	26	14	6
$[C_2F_4CN]^{+}$	126	1	1	18	22
$[C_2F_5CNH]^{+}$	146	4	3	6	2
$[C_2F_5CNH_2]^{+\cdot}$	147	<1	<1	<1	–
$[NHNH_2CC_2F_5]^{+\cdot}$	162	62	40	10	1
$[Ni(NHNHCC_2F_5)]^{+}$	219	1	1	2	–
$[Ni_2(NHNHCCF_3)(NH_3)]^{+}$	244	<1	<1	8	3
$[Ni(NHNHCC_2F_5)(HN{=}C{=}N)]^{+\cdot}$	260	<1	1	4	2
$[Ni(NHNHCC_2F_5)(HN{=}C{=}NH)]^{+}$	261	<1	<1	1	–
$[Ni(NHNH_2CC_2F_5)(HN{=}C{=}NH)]^{+}$	262	<1	<1	2	–
$[Ni(NHNH_2CC_2F_5)(CO_2)]^{+}$	264	<1	<1	4	2
$[Ni_2(NHNHCC_2F_5)(O_2CCF_3)_2(CF_3)]^{2+}$	286	–	–	3	1
$[Ni(CF_3)_2(C_2F_5)]^{+}$	315	–	<1	10	2
$[Ni(NHNHCC_2F_5)(O_2CCF_3)]^{+\cdot}$	332	4	2	–	–
$[Ni_2(NHNH_2CC_2F_5)(O_2CCF_3)_4\ \text{-H}]^{2+}$	364	<1	1	24	–
$[Ni(NHNHCC_2F_5)_2]^{+\cdot}$	380	2	1	–	–
$[Ni_2(NHNHCC_2F_5)_2(O_2CCF_3)]^{+\cdot}$	551	<1	–	1	–
$[Ni_2(NHNH_2CC_2F_5)(NHNHCC_2F_5)(O_2CCF_3)]^{+\cdot}$	552	–	<1	1	–

$[Ni_2(NHNH_2CC_2F_5)_2(O_2CCF_3)(NH_3)]^+$	570	–	–	4	1
$[Ni_2(NHNH_2CC_2F_5)(O_2CCF_3)_3]^+$	617	3	2	–	–
$[Ni_2(NHNH_2CC_2F_5)_3(NH_3)]^+$	619	1	1	19	4
$[Ni(NHNHCC_2F_5)_2(O_2CCF_3)_2(NH_3)_2(CO)]^+$	668	<1	2	32	24
$[Ni_2(NHNHCC_2F_5)_2(O_2CCF_3)_3]^+$	777	7	5	–	–
$[Ni_3(NHNH_2CC_2F_5)_3(O_2CCF_3)_2]^+$	888	–	–	–	–

Table S 7 EI MS results for the complex [$Ni_2(HAMDCF_3)_2(\mu\text{-}O_2CC_2F_5)_4$] (**3**).

Fragments	m/z	Relative Intensity (RI) [%]			
		441 K	458 K	496 K	573 K
$[F_2]^{+\cdot}$	38	<1	1	–	–
$[HN{=}C{=}N]^{+}$	41	1	1	–	–
$[HN{=}C{=}NH]^{+\cdot}$	42	4	3	–	–
$[CO_2]^{+\cdot}$	44	80	100	22	92
$[CO_2H]^{+}$	45	98	31	34	15
$[Ni]^{+}$	58	<1	2	–	–
$[CF_3]^{+}$	69	100	75	83	100
$[CF_2CN]^{+}$	76	4	11	7	–
$[CF_3CNH]^{+}$	96	5	4	–	–
$[CF_3CNH_2]^{+\cdot}$	97	38	10	13	7
$[C_2F_4]^{+}$	100	83	32	50	71
$[NHNH_2CCF_3]^{+\cdot}$	112	9	8	–	–
$[C_2F_5]^{+}$	119	68	26	36	40
$[C_2F_5CO_2H]^{+\cdot}$	164	<1	<1	–	–
$[Ni(NHNHCCF_3)]^{+}$	169	1	1	–	–
$[Ni(NHNH_2CCF_3)]^{+}$	170	1	3	–	–
$[Ni(NHNHCCF_3)(NCN)]^{+\cdot}$	209	2	1	–	–
$[Ni(NHNH_2CCF_3)(NCN)]^{+}$	210	1	1	–	–
$[Ni(NHNHCCF_3)(CF_3CN)]^{+}$	264	1	14	–	–
$[Ni(NHNHCCF_3)_2(NH_3)]^{+\cdot}$	297	–	–	5	1
$[Ni(O_2CC_2F_5)(CF_3NH)]^{+\cdot}$	305	–	1	–	–
$[Ni(NHNHCCF_3)(O_2CC_2F_5)]^{+\cdot}$	332	2	2	–	–
$[Ni_2(NHNHCCF_3)(O_2CC_2F_5)]^{+}$	390	–	<1	9	1
$[Ni_2(NHNH_2CCF_3)(O_2CC_2F_5)]^{+}$	391	–	<1	–	–
$[Ni_3(O_2CC_2F_5)(HNCNC)]^{+}$	392	–	<1	10	2
$[Ni_2(O_2CC_2F_5)_2]^{+\cdot}$	442	–	<1	19	4
$[Ni(NHNH_2CCF_3)_2(O_2CC_2F_5)]^{+}$	445	20	2	5	–
$[Ni_2(NHNH_2CCF_3)(NHNHCCF_3)_2]^{+\cdot}$	450	<1	2	–	–

$[Ni_2(NHNH_2CCF_3)(O_2CC_2F_5)(CF_3)]^{+\cdot}$	460	<1	1	27	17
$[Ni_2(NHNH_2CCF_3)(NHNHCCF_3)(O_2CCF_3)(NH_3)]^{+\cdot}$	469	2	17	–	–
$[Ni_2(NHNH_2CCF_3)_2(O_2CC_2F_5)(NH_3)]^{+}$	520	1	5	–	–
$[Ni_3(NHNH_2CCF_3)(NHNHCCF_3)_2(CN)]^{+}$	536	–	1	23	5
$[Ni_2(NHNHCCF_3)(O_2CC_2F_5)_2]^{+}$	553	<1	1	7	–
$[Ni_2(NHNHCCF_3)(NCCF_3)(O_2CC_2F_5)(C_2F_5)]^{+\cdot}$	604	1	2	–	–
$[Ni_2(O_2CC_2F_5)_3]^{+}$	605	<1	1	77	13
$[Ni_3(NHNH_2CCF_3)(O_2CC_2F_5)_2(NH_3)]^{+}$	629	–	1	6	–
$[Ni_3(NHNHCCF_3)_2(O_2CC_2F_5)(C_2F_5)]^{+}$	680	<1	2	86	21
$[Ni_2(NHNHCCF_3)(O_2CC_2F_5)_3]^{+\cdot}$	716	2	2	–	–
$[Ni_3(NHNHCCF_3)(O_2CC_2F_5)_3(NH_3)]^{+}$	793	–	–	–	5
$[Ni_2(NHNHCCF_3)_2(O_2CC_2F_5)_3]^{+}$	827	1	1	–	–
$[Ni_3(O_2CC_2F_5)_4(NH_3)]^{+}$	845	–	<1	13	46
$[Ni_3(O_2CC_2F_5)_5]^{+}$	989	–	<1	24	–
$[Ni_4(NHNHCCF_3)(O_2CC_2F_5)_3(CO_2)_4]^{+\cdot}$	1013	–	1	4	–
$[Ni_3(NHNH_2CCF_3)(NHNHCCF_3)_2(O_2CC_2F_5)_3(CF_3)(NH_3)]^{+\cdot}$	1085	–	<1	2	5

Table S 8 EI MS results for the complex $[Ni_2(HAMDC_2F_5)_2(\mu\text{-}O_2CC_2F_5)_4]$ (**4**).

Fragments	**m/z**	**Relative Intensity (RI) [%]**			
		324 K	**328 K**	**329 K**	**332 K**
$[HN{=}C{=}N]^+$	41	10	<1	–	–
$[HN{=}C{=}NH]^{+\cdot}$	42	20	1	1	3
$[CO_2]^{+\cdot}$	44	28	37	5	69
$[CO_2H]^{+\cdot}$	45	100	22	3	34
$[Ni]^+$	58	–	1	–	–
$[CF_3]^+$	69	32	25	5	100
$[CF_2CN]^+$	76	1	<1	<1	5
$[C_2F_4]^+$	100	18	16	4	80
$[C_2F_5]^+$	119	14	17	3	56
$[C_2F_4CN]^+$	126	–	–	<1	3
$[C_2F_5CNH]^+$	146	<1	2	<1	1
$[C_2F_5CNH_2]^+$	147	1	1	<1	6
$[NHNH_2CC_2F_5]^{+\cdot}$	162	3	3	1	13
$[C_2F_5CO_2H]^{+\cdot}$	164	3	9	–	–
$[Ni(NHNHCC_2F_5)]^+$	219	–	8	<1	1
$[Ni(NHNH_2CC_2F_5)]^+$	220	–	10	<1	–
$[Ni(O_2CC_2F_5)]^+$	221	–	4	<1	–
$[Ni(NHNHCC_2F_5)(HN{=}C{=}NH)]^+$	261	–	1	–	–
$[Ni(NHNH_2CC_2F_5)(HN{=}C{=}NH)]^+$	262	–	2	–	–
$[Ni(NHNH_2CC_2F_5)(NHNHCC_2F_5)]^+$	381	–	40	1	–
$[Ni(NHNHCC_2F_5)(O_2CC_2F_5)]^{+\cdot}$	382	–	16	<1	–
$[Ni_4(O_2CC_2F_5)(C_2F_5)(NH_3)]^+$	533	–	4	1	2
$[Ni(NHNH_2CC_2F_5)_2(O_2CC_2F_5)]^+$	545	–	13	1	–
$[Ni_2(NHNH_2CC_2F_5)_2(O_2CC_2F_5)]^+$ $[Ni_2(NHNHCC_2F_5)(O_2CC_2F_5)_2]^+$	603	–	15	2	1
$[Ni_2(O_2CC_2F_5)_3]^+$	605	–	12	2	2
$[Ni_2(NHNH_2CC_2F_5)_2(O_2CC_2F_5)_2]^{+\cdot}$ $[Ni_2(NHNHCC_2F_5)(O_2CC_2F_5)_3]^{+\cdot}$	766	–	–	–	1
$[Ni_2(NHNH_2CC_2F_5)(O_2CC_2F_5)_3]^+$	767	–	6	33	–
$[Ni_2(NHNHCC_2F_5)_2(O_2CC_2F_5)_2(CO_2)]^{+\cdot}$	808	–	1	3	–

$[Ni_2(NHNH_2CC_2F_5)(HN{=}C{=}NH)(O_2CC_2F_5)_3]^+$	809	–	<1	–	–
$[Ni_3(NHNHCC_2F_5)(O_2CC_2F_5)_3(NH_3)]^+$	843	–	1	7	–
$[Ni_2(NHNH_2CC_2F_5)(NHNHCC_2F_5)(O_2CC_2F_5)_3]^{+\cdot}$	928	–	9	–	–
$[Ni_2(NHNH_2CC_2F_5)_2(O_2CC_2F_5)_3(CC_2F_5)]^{+\cdot}$	1060	–	<1	6	–
$[Ni_4(NHNH_2CC_2F_5)(O_2CC_2F_5)_3(CO_2)_4]^+$	1061	–	<1	10	1

Table S 9 EI MS results for the complex $[Ni(IMAMDCF_3)_2]$ (**5**).

Fragments	**m/z**	**Relative Intensity (RI) [%]**		
		332 K	**334 K**	**339 K**
$[CH_3CN]^{+\cdot}$ / $[HN{=}C{=}N]^+$	41	2	–	15
$[NH{=}C{-}NH]^{+\cdot}$	42	1	–	41
$[NH{=}C{-}NH_2]^{+\cdot}$	43	2	3	43
$[CF_2]^+$	50	12	7	16
$[Ni]^+$	58	2	2	45
$[CF_3]^+$	69	90	62	100
$[CF_2CN]^{+\cdot}$	76	8	3	–
$[Ni(HN{=}C{=}NH)]^+$	100	2	6	2
$[N_2CCF_3]^+$	109	–	–	3
$[NHNHCCF_3]^+$	111	–	–	3
$[NHNH_2CCF_3]^{+\cdot}$	112	–	–	–
$[C_2F_4CN]^+$	126	–	–	3
$[Ni(NCCF_3)]^+$	153	1	5	–
$[Ni(NHNH_2CCF_3)]^+$	170	3	11	2
$[Ni(NHCNCNH)_2]^{+\cdot}$	194	2	9	2
$[Ni(NHCNCNH)_2(NH_3)]^{+\cdot}$	211	8	18	4
$[Ni(NH_2CNCNH)_2(NH_3)_2]^{+\cdot}$	230	75	53	9
$[Ni(CF_3NCCF_3N)]^+$	236	11	10	–
$[Ni(NHC(CF_3)NC(CF_3)NH)]^+$	264	3	13	3
$[Ni(NH_2C(CF_3)NC(CF_3)NH)]^+$	265	14	66	13
$[Ni(CNC(CF_3)NC(CF_3)NC)]^+$	286	48	40	3
$[Ni(NHC(CF_3)NC(CF_3)NH)(NHC(CF_3)NCCF_2N)]^{+\cdot}$	450	–	–	2
$[Ni(NHC(CF_3)NC(CF_3)NH)_2]^{+\cdot}$	470	18	99	24

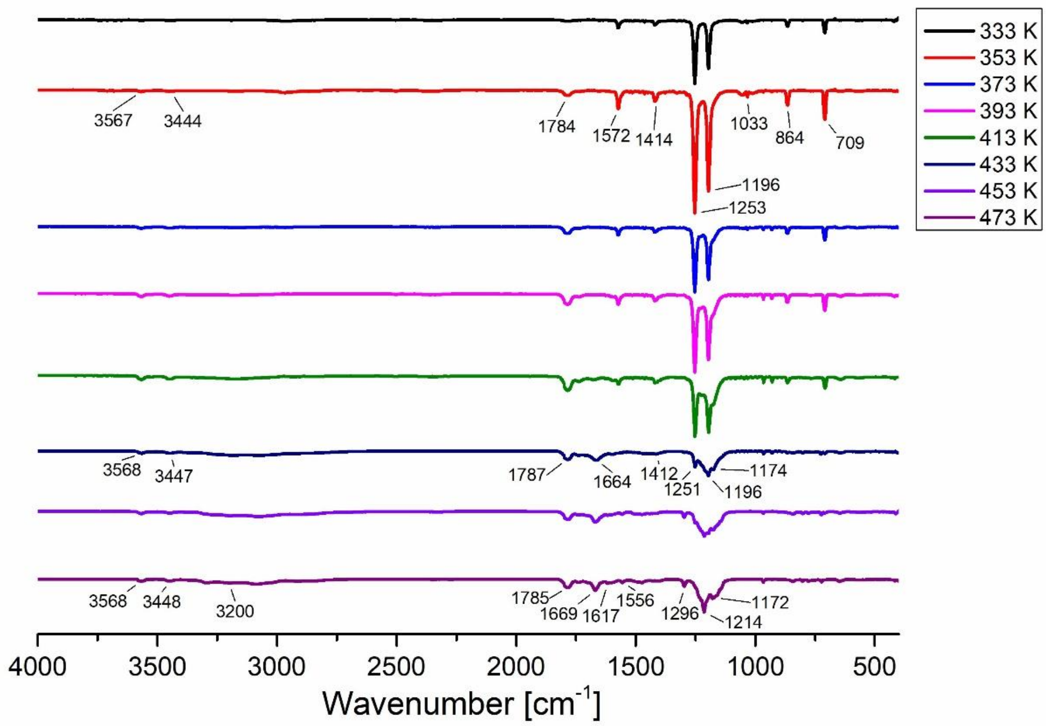

Figure S 15 Temperature variable infrared spectra VT IR for the vapor formed during the [$Ni_2(HAMDCF_3)_2(\mu\text{-}O_2CCF_3)_4$] (**1**) heating (333−473 K).

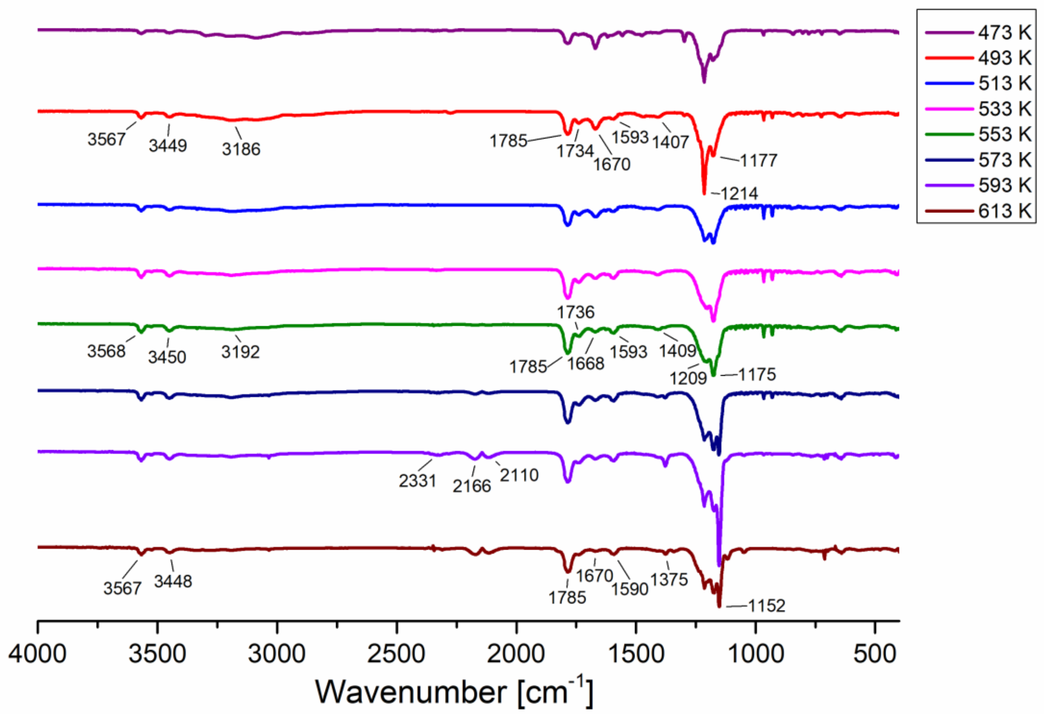

Figure S 16 Temperature variable infrared spectra VT IR for the vapor formed during the [$Ni_2(HAMDCF_3)_2(\mu\text{-}O_2CCF_3)_4$] (**1**) heating (473−613 K).

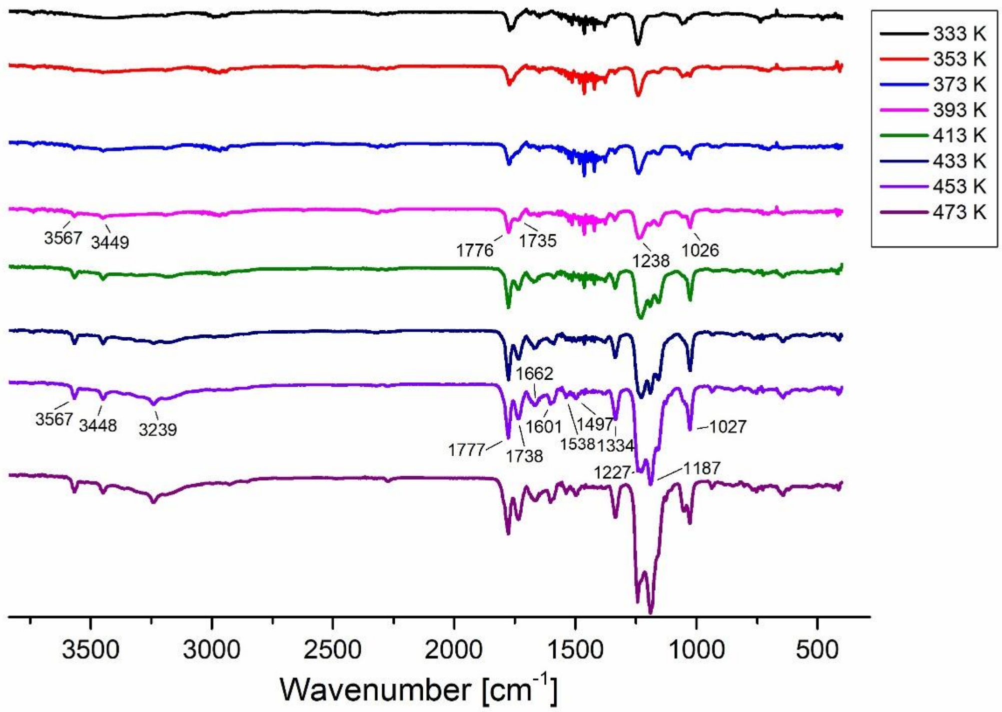

Figure S 17 Temperature variable infrared spectra VT IR for the vapor formed during the [$Ni_2(HAMDC_2F_5)_2(\mu\text{-}O_2CCF_3)_4$] (**2**) heating (333−473 K).

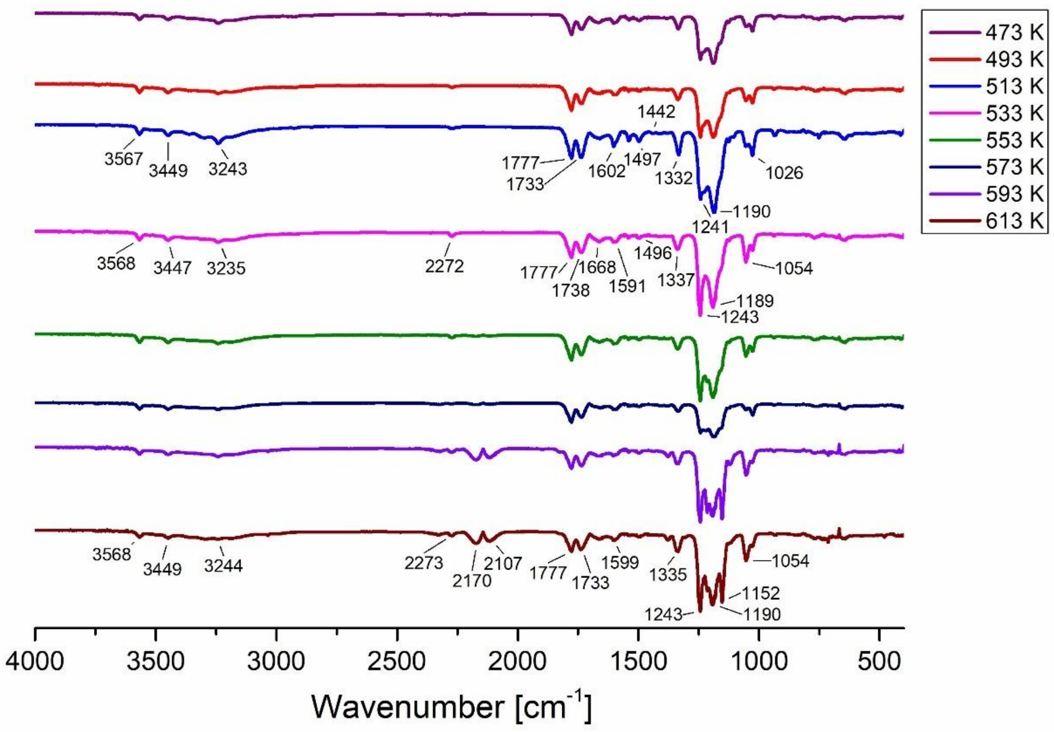

Figure S 18 Temperature variable infrared spectra VT IR for the vapor formed during the [$Ni_2(HAMDC_2F_5)_2(\mu\text{-}O_2CCF_3)_4$] (**2**) heating (473−613 K).

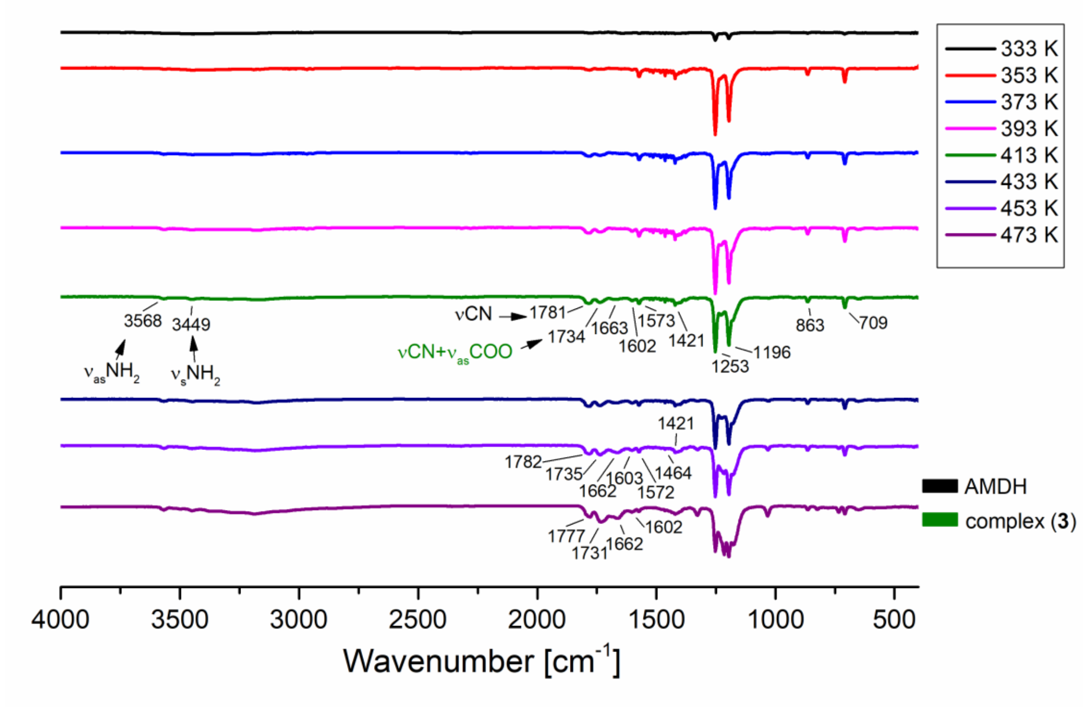

Figure S 19 Temperature variable infrared spectra VT IR for the vapor formed during the [$Ni_2(HAMDCF_3)_2(\mu\text{-}O_2CC_2F_5)_4$] (**3**) heating 333−473 K (bands characteristic for: free HAMD – black, complex – green).

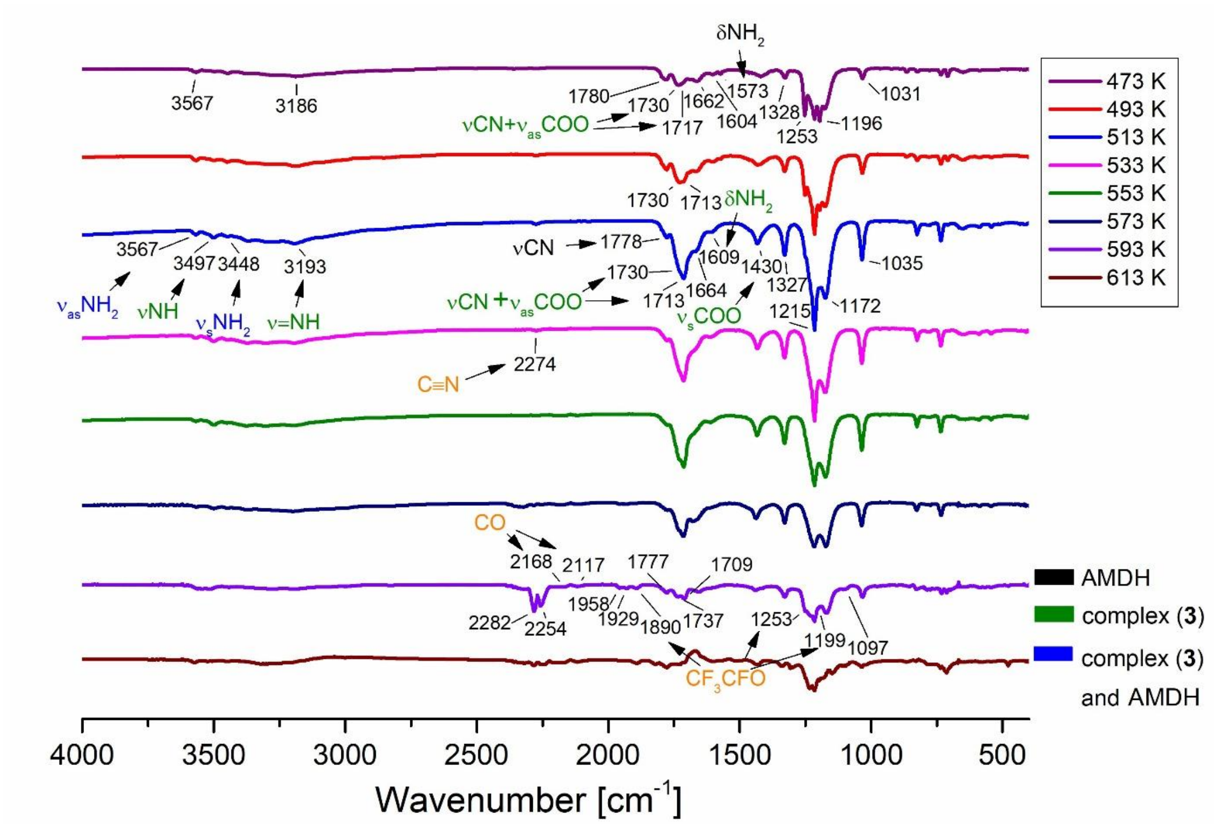

Figure S 20 Temperature variable infrared spectra VT IR for the vapor formed during the [$Ni_2(HAMDCF_3)_2(\mu\text{-}O_2CC_2F_5)_4$] (**3**) heating 473−613 K (bands characteristic for: free HAMD – black, complex – green, complex and HAMD – blue assignment).

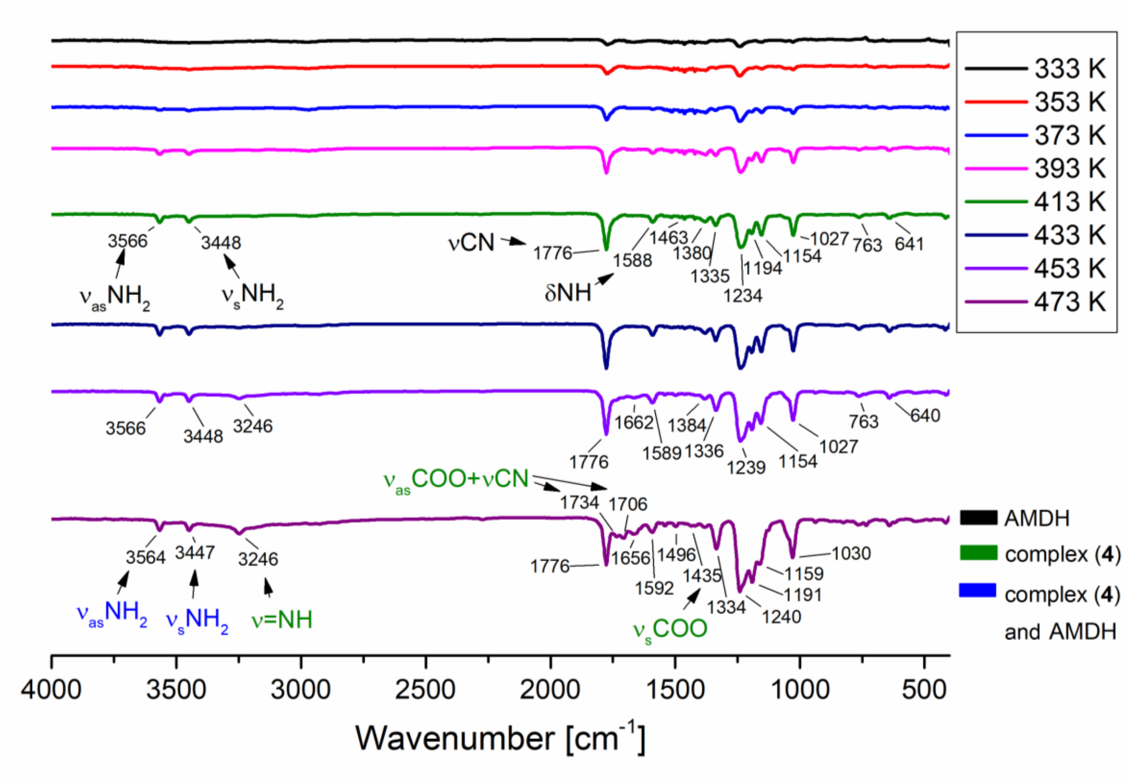

Figure S 21 Temperature variable infrared spectra VT IR for the vapor formed during the $[Ni_2(HAMDC_2F_5)_2(\mu\text{-}O_2CC_2F_5)_4]$ (**4**) heating 333−473 K (bands characteristic for: free HAMD – black, complex – green, complex and HAMD – blue assignment).

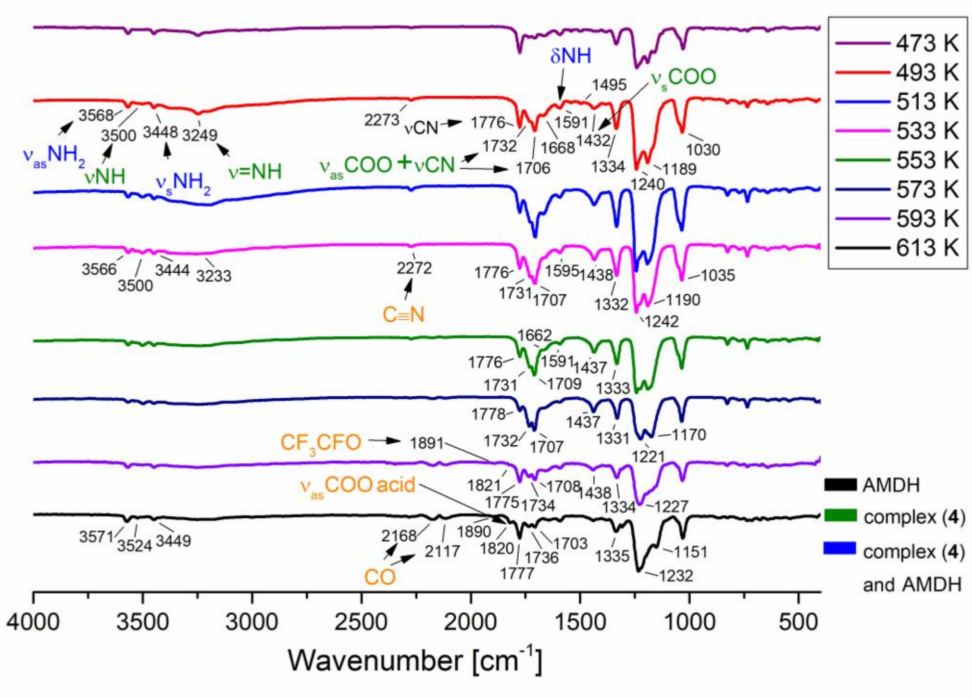

Figure S 22 Temperature variable infrared spectra VT IR for the vapor formed during the $[Ni_2(HAMDC_2F_5)_2(\mu\text{-}O_2CC_2F_5)_4]$ (**4**) heating 473−613 K (bands characteristic for: free HAMD – black, complex – green, complex and HAMD – blue assignment).

Table S 10 Vibrational band positions and assignments for gaseous products of thermal decomposition of [$Ni_2(HAMDR_f)_2(\mu\text{-}O_2CC_2F_5)_4$] (**3**) and [$Ni_2(HAMDR_f)_2(\mu\text{-}O_2CC_2F_5)_4$] (**4**), where $R_f = CF_3$ (**3**), C_2F_5 (**4**).

Assignement (ca.) [cm^{-1}]	**(1)**	**(2)**	**(3)**	**(4)**
νC≡N *($R_fC≡N$)*	–	2273	2272	2274
νCO *(CO)*	2166 2110	2170 2107	2168 2117	2168 2117
νCO_2	2331	–	–	–
ν$_{as}$COO *(acid)*	–	–	1820	–
νC=O *(CF_3CFO)*	–	–	–	1890
νCF *(CF_3CFO)*	–	–	–	1253 1199

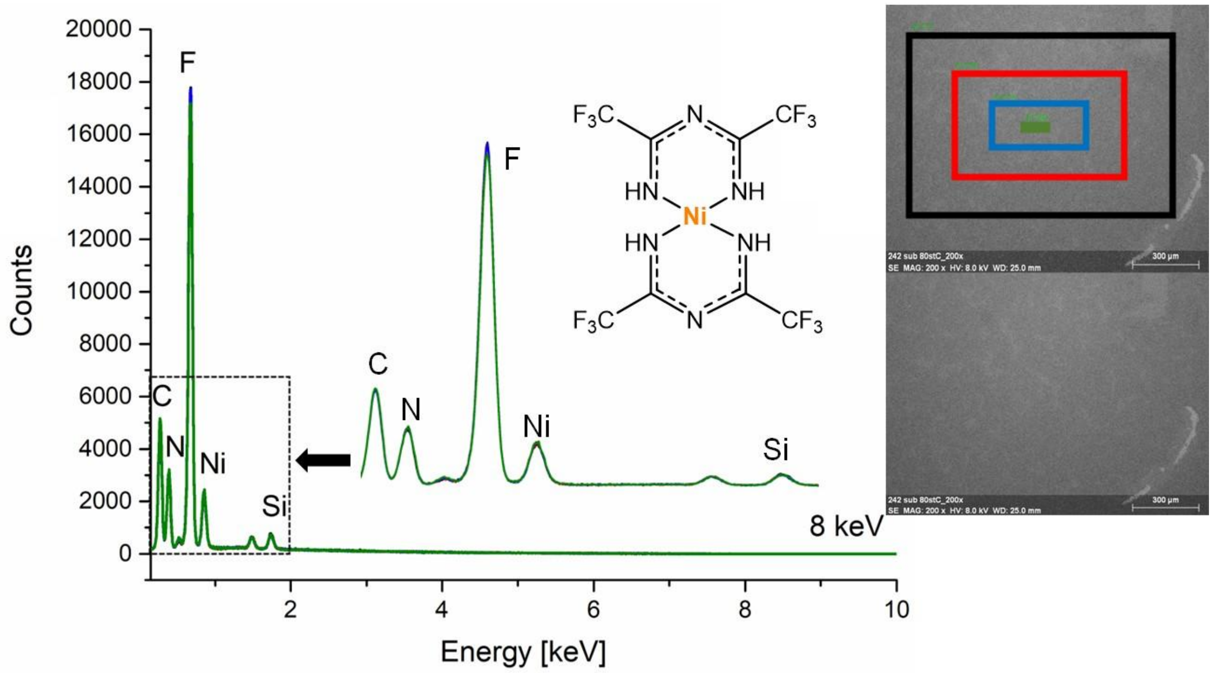

Figure S 23 Examined scan areas' EDX spectra (8 keV) for the [$Ni(IMAMDCF_3)_2$] (**5**) layer deposited on a Si(111) substrate (Mag = 200x).

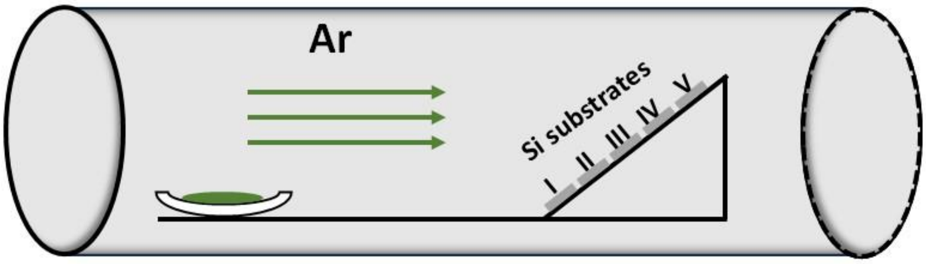

Figure S 24 CVD reactor scheme with marked substrates, numbered according to the length of the transport path.

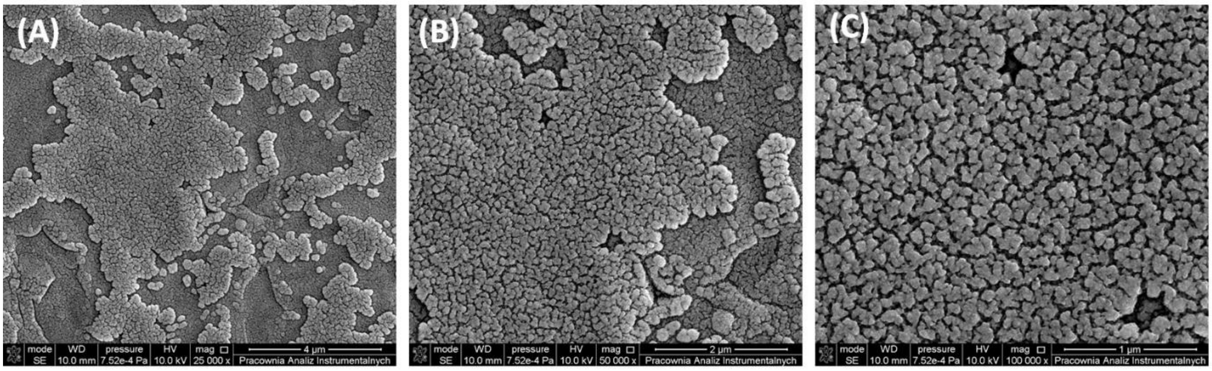

Figure S 25 SEM images of deposits formed using the precursor $[Ni_2(HAMDC_2F_5)_2(\mu\text{-}O_2CC_2F_5)_4]$ (**4**) (T_V = 493 K, T_D = 723 K, Ar), on titania nanotubes, (A) − Mag = 25000x, (B) – Mag = 50000x, (C) – 100000x.

Table S 11 The k_{obs} values for methylene blue photocatalytic degradation under UV-lamp without (REF) and with TNT20 or Ni-TNT20 substrates as catalysts. Repetitions were carried out using the same substrates.

Substrate	Test number	10^9 k_{obs} [Ms^{-1}]
REF	1	0.44 ± 0.11
	2	0.21 ± 0.01
	3	0.43 ± 0.15
TNT20	1	2.14 ± 0.16
	2	1.63 ± 0.09
	3	0.91 ± 0.02
Ni-TNT20	1	3.39 ± 0.27
	2	1.73 ± 0.10
	3	0.94 ± 0.13

Table S 12 The k_{obs} values for methylene blue photocatalytic degradation under Vis-lamp without (REF) and with TNT20 and Ni-TNT20 substrates as catalysts.

Substrate	10^9 k_{obs} [Ms^{-1}]
REF	0.35 ± 0.04
TNT20	0.23 ± 0.03
Ni-TNT20	0.33 ± 0.07

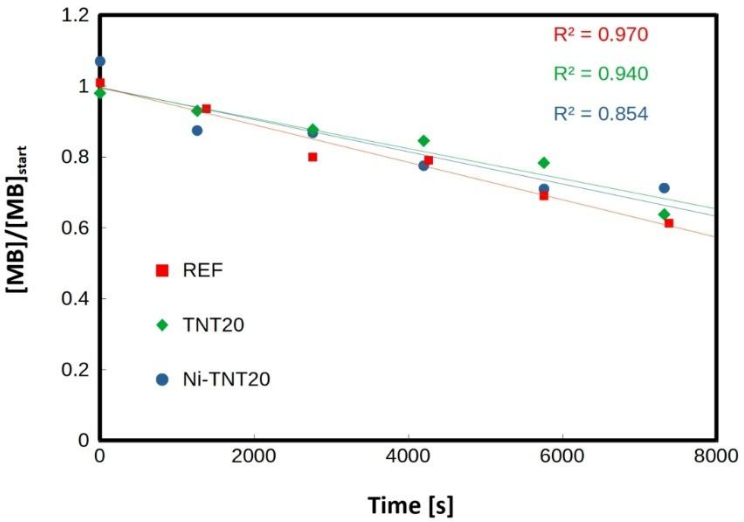

Figure S 26 The absorbance-time dependencies for the studied substrates (TNT20 and Ni-TNT20) and the sample without the substrate (REF) during the Vis irradiation. $[MB]_0 = 1 \cdot 10^5$ mol/dm^3, T = 298.1 K.